Anisotropic water reorientation around ions

K.J. Tielrooij,[1, 2] S.T. van der Post,[1] J. Hunger,[1] M. Bonn,[1] and H.J. Bakker[1]

[1]*FOM Institute for Atomic and Molecular Physics [AMOLF]*
*Science Park 104, 1098 XG Amsterdam, The Netherlands*
[2]*Currently at ICFO – Institut de Ciencies Fotoniques,*
Mediterranean Technology Park, 08860 Castelldefels (Barcelona), Spain

We study the reorientation dynamics of water molecules around ions using terahertz dielectric relaxation spectroscopy and polarization-resolved femtosecond infrared pump-probe spectroscopy. The results are discussed in relation to the ion-specific Hofmeister series and the concomitant 'structure making' and 'structure breaking' effects of ions on water. We show that, when a dissolved salt consists of a strongly hydrated ion with a weakly hydrated counterion, the reorientation of water molecules around the strongly hydrated ion is anisotropic, in the sense that differently charged ions affect reorientation along different molecular axes: cations mainly slow the reorientation dynamics of the water dipole vectors and anions mainly slow down the reorientation dynamics of the hydroxyl group that points towards the anion. In both cases, motion along only one molecular axis is impeded, so that the hydration shell is best described as semi-rigid. In this semi-rigid hydration picture water molecules in the first hydration shell show anisotropic reorientation, whereas water molecules outside the first hydration shell remain unaffected. The inferred anisotropy in molecular motion explains why terahertz dielectric relaxation spectroscopy, which probes dipolar relaxation, is more sensitive to cation hydration effects while femtosecond infrared pump-probe spectroscopy, which is sensitive to reorientation of hydroxyl groups, is more sensitive to anion hydration effects. We also show that dissolution of CsI - a salt for which both cation and anion are weakly hydrated - has little effect on water reorientation dynamics, with hydration water displaying dynamics that are similar to those in bulk water.

I. INTRODUCTION

The behavior of biomolecules in aqueous solution is affected by the presence of specific ions in that solution. For example, the solubility of proteins depends strongly on the ions that are present in the solution. This effect is highly ion-specific and lies at the origin of the Hofmeister series, which dates back to the late 19th century [12, 22]. An (incomplete) ordering of the strength of the effect of ions on a biomolecular solution, is given as [8]:

$$F^- > Cl^- > I^- > ClO_4^- \quad \text{(anions)}$$
$$Mg^{2+} < Li^+ < Na^+ < Cs^+ \quad \text{(cations)}.$$
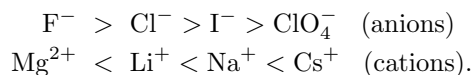
Here, ions on the left end are typically strongly hydrated and on the right typically weakly hydrated, where the degree of hydration indicates the extent to which water molecules around these ions are affected in their structure and dynamics. The degree of hydration typically increases with decreasing ion radius and increasing ion charge. It turns out that strongly hydrated anions and weakly hydrated cations lead to increased surface tension, decreased hydrocarbon solubility, aggregation effects (salting out) and an increased protein stability. These ion-specific interactions are commonly encountered in many different (biologically relevant) systems [22, 30, 44].

At present, there is an ongoing discussion whether the Hofmeister series result from direct interactions between ions and biomolecular species [49] or from a (long-range) interaction between the ions and water molecules (asso-ciated with 'structure making' and 'structure breaking'), which in turn affects the properties of the solution [44]. For this discussion it is imperative to first understand how ions affect the structure and the dynamics of the surrounding water molecules and what the range of this effect is. In a recent spectroscopic study of the dynamics of water molecules in solutions with different salts, it was shown that a cooperative effect occurs when strongly hydrated ions and counterions (such as Mg^{2+} and SO_4^{2-}) are combined. The combination of these ions leads to very rigid hydration structures between the ions, which extend well beyond their first hydration shell. The observed cooperativity in ion hydration has implications for the Hofmeister series: it shows that the Hofmeister series should be considered in terms of salts, instead of individual ions [50]. Hence, the molecular origin of the Hofmeister series could be related to cooperative 'structure making' effects between strongly hydrated cations, e.g. Mg^{2+} and Ca^{2+}, and biomolecules, e.g. DNA and proteins, which contain negative charges. Due to this cooperativity between ions and biomolecules, the water dynamics are affected, which in turn leads to changes in the properties of the solution. This explanation of the molecular origin of the Hofmeister series forms an alternative to either direct ion-biomolecule interaction effects or to the effects of the ions on water.

Here, we investigate in more detail the effects of ions on water, by studying the water reorientation dynamics around positively and negatively charged ions. This study is performed in comparison with the dynamics of water around hydrophobic species. We have chosen

the salts CsF and LiCl, which consist of a strongly hydrated monovalent ion (F^- and Li^+ respectively), combined with a weakly hydrated counterion (Cs^+ and Cl^-, respectively), such that no (or only very weak) cooperative effects are expected. We also study water reorientation dynamics around CsI, a salt where both the anion and the cation are known to be weakly hydrated, in order to examine if this would lead to a speedup of water dynamics. This could be expected since 'weakly hydrated' is often equated to 'structure breaking'. We use two techniques that provide access to the ultrafast water reorientation dynamics, namely terahertz dielectric relaxation (THz-DR) spectroscopy and femtosecond infrared (fs-IR) spectroscopy. Both techniques are sensitive to the same reorientation process in neat water and have shown over the last years to be powerful tools for investigating water dynamics [16, 28, 31, 34, 37, 47, 48] and extracting dynamic hydration effects [14, 17, 20, 32, 33, 43].

II. EXPERIMENTAL AND ANALYSIS

A. Samples

The samples were solutions of different salts in Millipore-purified water (resistivity >18 MΩ/cm). For the THz-DR measurements, we used the salts CsF, LiCl, CsI and CsCl, all up to a concentration of about 1 mol/kg. These salts have the following known conductivities due to ion mobility at 1 mol/kg: CsF 8.48 S/m [27], LiCl 7.45 S/m [45], CsI 11.87 S/m [13] and CsCl 10.873 S/m [7]. For the fs-IR measurements, the salts were dissolved in pure water that contained 4% (vol.) D_2O and 96 % H_2O, up to 4 mol/kg for CsF and LiCl, and up to 2 mol/kg for CsI (restricted by solubility). All experiments were carried out at room temperature and under standard pressure.

B. Terahertz dielectric relaxation spectroscopy

Dielectric relaxation spectroscopy is a very powerful technique to examine the reorientation dynamics of polar molecules over a wide range of frequencies, traditionally up to the GHz range. This technique relies on the interaction between a molecule with a permanent dipole and an external AC electric field, which exerts an aligning force on the dipole (with an energy smaller than the thermal energy). Molecular reorientation processes lead to a characteristic frequency dependence of the dielectric function, i.e. dielectric relaxation. The occurrence of dielectric relaxation modes allows for the determination of the reorientation time constants and a quantification of the number of involved molecules. Dielectric relaxation modes are distinct from modes with

a nonzero resonance frequency (resonance modes) [2] and are intrinsically broad. Thus, an accurate description of dielectric relaxation modes requires adequate experimental frequency coverage [9], up to the - until recently experimentally challenging - THz regime.

The THz dielectric relaxation measurements, which we describe below and in more detail in the Appendix, probe directly the reorientation dynamics of water dipoles through the frequency dependence of the complex dielectric function up to a frequency of ∼1.2 THz. From the reduction of the dielectric response, the number of water molecules with slower dynamics is extracted. This low-frequency THz dielectric relaxation technique is complementary to the approach of Havenith et al. who use a p-Ge laser that produces THz radiation in the range 2.3-2.8 THz (75-100 cm^{-1}) [38], and to the time-domain coherent Raman scattering technique of Meech et al. with frequency coverage up to 15 THz (500 cm^{-1}) [10]. At these higher THz frequencies, one does not probe the dielectric relaxation modes of water due to dipolar reorientation (as in our THz-DR technique), but resonance modes that are ascribed to a concerted motion involving the second solvation shell peaked at ∼2.4 THz [11], rattling modes of ions within the water network with ion-dependent peaks between 2.4 and 5.7 THz [38] and hydrogen bond vibrations that occur between 3.8 and 5.3 THz [10]. The upper limit of 1.2 THz for our spectral range is based on Ref. [9], where the dielectric loss and the Raman spectrum of water were analyzed from the MHz region up to 18 THz and described by two dielectric relaxation modes and four damped harmonic oscillators corresponding to resonant modes.

1. THz-DR setup

We perform dielectric relaxation spectroscopy using a terahertz time-domain spectroscopy setup. Light in the terahertz frequency range is generated through optical rectification in ZnTe, using 800 nm pulses from a Ti:Sapphire amplified laser system with a 1 kHz repetition rate. The 800 nm pulses have a duration of ∼150 fs and a pulse energy of ∼70 µJ and produce single-cycle THz pulses with a center frequency around 0.6 THz and a peak electric field strength of 1 kV/cm. The 800 nm beam that creates the THz radiation passes through a 500 Hz chopper for active background subtraction. The time-dependent quasi-instantaneous electric field strength of the THz pulses is measured by means of electro-optic sampling with a variably delayed detection pulse of 800 nm light (duration ∼150 fs). The detection scheme is based on the electro-optic effect in a second ZnTe crystal: the 800 nm detection pulse undergoes a polarization change when it passes through the ZnTe crystal when the electric field from the THz pulse is present. By changing the arrival time of the

detection pulse with respect to the THz pulse using a variable optical delay line, the electric field strength of the complete THz time trace is mapped by polarization rotation of the much shorter 800 nm pulse.

2. Extracting the dielectric response

We determine the refraction and absorption that occur in the sample by comparing THz time traces transmitted through an empty cuvette with THz time traces transmitted through a cuvette that contains a sample, as refraction leads to a delayed THz pulse and absorption leads to a smaller pulse amplitude. The refractive and absorptive properties of a sample are expressed in the complex refractive index $\hat{n} = n - i\kappa$. Here n is the regular refractive index and κ is the extinction coefficient. The complex refractive index is related to the complex dielectric response $\hat{\epsilon} = \hat{n}^2 = \epsilon' - i\epsilon''$. As the THz pulses cover a frequency region $\nu = 0.2$–2 THz, we obtain the frequency-dependent complex dielectric function $\hat{\epsilon}(\nu)$ for these frequencies. See the Appendix for details on the extraction of the complex dielectric function.

We describe the dielectric response of aqueous salt solutions using the well-known double-Debye dielectric relaxation model [4, 6, 37]

$$\epsilon(\nu) = \frac{S_1}{1 + i2\pi\nu\tau_D} + \frac{S_2}{1 + i2\pi\nu\tau_2} + \frac{\sigma}{i2\pi\nu\epsilon_0} + \epsilon_\infty \ , \quad (1)$$

where the first term describes the dielectric relaxation mode with relaxation strength $S_1 = \epsilon_s - \epsilon_1$ and (Debye) reorientation time τ_D. The second mode has a (much smaller) relaxation strength $S_2 = \epsilon_1 - \epsilon_\infty$ and reorientation time τ_2. For pure water under ambient conditions, the first, slow Debye mode is centered at 20 GHz, whereas the second, faster mode has its maximum near 0.6 THz. The last term in equation (1) describes the contribution to the dielectric response of the ion conductivity σ, for which we use the literature values mentioned above. We also use literature data from Ref. [7] for the static permittivity ϵ_s of the reference sample (CsCl) that is measured in parallel with the sample of interest (LiCl, CsF or CsI). The measurement of the reference sample enables the calibration of the dielectric response of the sample under study (see the Appendix for the details on how the calibration is carried out).

3. Obtaining the slow water fraction (THz-DR)

The relaxation strength $S = S_1 + S_2$ reflects the number of water molecules that participate in reorientation, as the relaxation strength is linear in dipole concentration. The dielectric response of the sample at ion concentration c, $S(c) = S_1(c) + S_2(c)$, is typically smaller than the bulk water strength $S(0)$, leading to a negative polarization change $\Delta S(c) = S(c) - S(0)$. This depolarization is caused by three effects: (i) the ions take up space, making the effective water concentration of the solution lower than in the pure water case (dilution effect); (ii) due to ions that move in the driving field, water molecules are caused to reorient in a direction opposite to the driving field (kinetic depolarization), and (iii) due to the electric fields of the ions, some water molecules that are close to the ions are tightly bound and oriented, and as a result no longer participate in the bulk-like relaxation process (static depolarization). These molecules will show a much slower reorientation.

To determine the number of slowly reorienting water molecules involved in effect (iii), we first correct the measured depolarization for the kinetic depolarization contribution (ii) to obtain the static depolarization $\Delta S'(c)$ (keeping in mind that the depolarization is negative) [6, 15]

$$\Delta S'(c) = \Delta S(c) + \sigma(c) \cdot \frac{2\tau_D(0)}{3} \frac{\epsilon_s(0) - \epsilon_\infty(c)}{\epsilon_s(0)\epsilon_0} \ . \quad (2)$$

Here, $\epsilon_s(0)$ is the static permittivity of pure water and $\epsilon_\infty(c)$ the high frequency limit of the permittivity for the salt solution. The factor $^2/_3$ arises from the assumption of slip boundary conditions [6]. Then we obtain the slow water fraction using

$$f_{\text{slow}}^{\text{THz-DR}}(c) = 1 - \frac{S(0) + \Delta S'(c)}{S(0)} \frac{c_{\text{H}_2\text{O}}(0)}{c_{\text{H}_2\text{O}}(c)} \times \frac{[2\epsilon_s(c) + 1]\epsilon_s(0)}{\epsilon_s(c)[2\epsilon_s(0) + 1]} \ , \quad (3)$$

In this equation, $c_{\text{H}_2\text{O}}(c)$ is the concentration of solvent water molecules at salt concentration c in mol/L; $c_{\text{H}_2\text{O}}(0) = 55$ mol/L. With this equation, the dilution contribution, effect (i), to the depolarization $\Delta S'(c)$ is accounted for. The last factor is a correction that takes into account the local field effects (upon entering a medium with a lower permittivity, electric field lines become more dense), which only becomes significant at large depolarizations (high concentrations). If there is relatively more depolarization than due to the decrease of the water concentration and the kinetic depolarization, there is a fraction of water molecules that no longer takes part in bulk-like reorientation, i.e. these water molecules reorient more slowly. The remainder of the depolarization effect thus defines the fraction of slowly reorienting water $f_{\text{slow}}^{\text{THz-DR}}$. We note that Eq. 3 relies on the reasonable assumption that the size of the effective water dipole moments is not affected by the solute. Finally, the slope of the slow water fraction $f_{\text{slow}}^{\text{THz-DR}}(c)$ as a function of concentration c defines the THz-DR hydration number of a solvated salt $N^{\text{THz-DR}}$: the number

of moles of water molecules per mole dissolved salt, that no longer participate in bulk-like reorientation dynamics.

C. Femtosecond infrared pump-probe spectroscopy

The second technique used here that is sensitive to molecular reorientation, is polarization-resolved femtosecond mid-infrared vibrational (fs-IR) spectroscopy. This technique allows the direct study of the reorientational dynamics of water molecules with high temporal resolution ($\sim$150 fs). In these experiments, we excite the OD-stretch vibration of a subset of HDO molecules in H_2O (4% D_2O in H_2O) with an intense pump pulse from the vibrational ground state $v = 0$ to the first excited state $v = 1$. This excitation results in a bleaching of the fundamental $v = 0 \rightarrow 1$ transition, and an induced absorption at the frequency of the excited-state absorption $v = 1 \rightarrow 2$ transition. The latter absorption is redshifted by $\sim$200 cm^{-1} with respect to the fundamental transition due to the anharmonicity of the OD stretch vibration. Molecules with their OD group preferentially aligned along the polarization axis of the excitation (pump) pulse are most efficiently excited. Hence, the excitation by the pump pulse results in an anisotropic distribution of excited HDO molecules. After an adjustable delay, we probe the sample using a weak probe pulse, which has a polarization parallel or perpendicular to the pump pulse. A comparison of the two signals allows us to extract the number of excited OD groups that are oriented parallel and perpendicular to the excitation axis as a function of pump-probe delay time. The appropriately normalized difference between the perpendicular and parallel signal finally results in a time trace that represents the reorientation dynamics of the excited OD groups.

1. fs-IR setup

Part of the 800 nm light from a Ti:Sapphire laser is used to pump a white-light seeded OPA (Spectra-Physics). The resulting idler pulses, with a wavelength of 2000 nm, are doubled in a BBO crystal, and the resulting pulses with a wavelength of 1000 nm are passed through a $KNbO_3$ (KN) crystal, simultaneously with the remaining 800 nm light from the laser. Through difference-frequency mixing, infrared light with a wavelength of 4 μm (corresponding to a frequency of 2500 cm^{-1} or 75 THz) is created. After passing through a long-wave pass filter, the infrared light ($\sim$4 μJ) passes through a wedged CaF_2 window, where the transmitted light ($\sim$90%) is used as the pump; the light reflected from the front of the wedge is used as the probe; the light reflected from the back is used as reference. The pump polarization is rotated by 45° with respect to the

probe and reference using a $\lambda/2$ plate and focused in the sample (contained between two CaF_2 windows separated by a spacer with a thickness around 25 μm), using a parabolic mirror. The pump beam passes through a 500 Hz chopper in order to increase the sensitivity towards pump-induced changes in the absorption of the sample. The probe light passes through a variable delay line, before being focused on the same spot in the sample as the pump light. With the delay line, the timing can be tuned such that the probe arrives before (t negative) or after the pump pulse (t positive). The reference beam, used to correct for pulse to pulse intensity fluctuations, is focused at a different spot in the sample. After passing through the sample, the pulses pass through a polarizer, which rotates between two positions, thereby selecting the polarization component of the probe that is parallel to the pump polarization or the polarization component of the probe that is perpendicular to the pump polarization. The probe and reference beams are spectrally dispersed by a grating in a spectrograph, and detected with a 2$\times$32 pixel liquid-nitrogen cooled HgCdTe (MCT) detector (Infrared Associates). The data present the pump-induced change in absorption $\Delta\alpha(t,\nu)$ of the sample at each frequency pixel ν for different time delays t for the two polarizations $\parallel$ and $\perp$.

2. Extracting the anisotropy decay

To extract the water reorientation dynamics from the data, we first need to correct the signals for the ingrowing heat effect: the relaxation of the excited OD vibrations results in a heating of the the sample (typically by $\sim$ 1° C). The heating leads to a transient absorption change that adds to the signal of the bleaching of the fundamental $v = 0 \rightarrow 1$ OD transition. As the heated sample has a blue-shifted OD-stretch absorption spectrum, the pump-induced absorption change at long delay times is nonzero and this signal grows in with a similar (picosecond) time scale as the water reorientation dynamics. To obtain the anisotropy dynamics of the bleaching signal only, the ingrowing heat spectrum, which we take to be isotropic, needs to be subtracted. To obtain the heat ingrowth dynamics, we use a cascading model with one intermediate state, as in Ref. [34]. After subtracting the time-dependent heat signal, we obtain the pump-induced changes in OD absorption for pump and probe polarizations mutually parallel and perpendicular: $\Delta\alpha'_{\parallel}(t,\nu)$ and $\Delta\alpha'_{\perp}(t,\nu)$. These heat-corrected absorption changes are used to construct the anisotropy $R(t,\nu)$ as a function of pump probe delay time t

$$R(t,\nu) = \frac{\Delta\alpha'_{\parallel}(t,\nu) - \Delta\alpha'_{\perp}(t,\nu)}{\Delta\alpha'_{\parallel}(t,\nu) + 2\Delta\alpha'_{\perp}(t,\nu)} \quad . \qquad (4)$$

The denominator in this equation is equal to the isotropic signal, i.e. the rotation-independent signal. We average

the anisotropy decay over a range of frequencies to obtain the anisotropy decay as a function of pump-probe delay time $R(t)$. The anisotropy decay is directly proportional to the (second-order) orientational correlation function and reflects the reorientation dynamics of all HDO molecules that have an OD-vibration absorbing in the probed frequency range. For reasons specified below, we use a slightly red-shifted excitation and probe pulse that is centered around 2480 cm^{-1}.

3. Obtaining the slow water fraction (fs-IR)

In aqueous salt solutions, we describe the anisotropy decay using a bimodal model, which identifies two distinct species: one with reorientation dynamics that are largely unaffected or bulk-like, and one with slower reorientation dynamics. The slow time constant and the associated fraction of slow hydration shell water are obtained from a double exponential fit to the anisotropy decay. Here the bulk-like time constant is determined from independent measurements of the reorientation time of neat water ($\tau_{\text{bulk}} = 2.6 \pm 0.1$ ps at room temperature). The slow component represents a weighted average of water molecules that have in common that they reorient more slowly than the water molecules in bulk liquid water. Hence, we fit the data to the following equation:

$$R(t) = A_{\text{bulk}} \cdot e^{-t/\tau_{\text{bulk}}} + A_{\text{slow}} \cdot e^{-t/\tau_{\text{slow}}} \ . \qquad (5)$$

The data were found to be best described with a slow water time constant of $\tau_{\text{slow}} = 10\text{–}20$ ps, which corresponds to typical values found for the residence time of water molecules in the solvation shells of ions [18]. In analogy to the DR measurements, we extract the slow water fraction as measured with fs-IR spectroscopy

$$f_{\text{slow}}^{\text{fs–IR}} = \frac{A_{\text{slow}}}{A_{\text{bulk}} + A_{\text{slow}}} \ . \qquad (6)$$

This slow water fraction can be translated into a hydration number $N^{\text{fs–IR}}$ by multiplying the fraction with $\frac{2c_{H_2O}}{c}$, which gives the number of moles of slowly reorienting OD groups per mole of dissolved salt. The factor 2 arises because there are two OD groups per water molecule. For instance, in case there are 6 slow OD groups per cation + anion pair, the fraction slow water for a $c = 1$ mol/L salt solution will be 6/110 ($2c_{H_2O} = 110$ mol/L), and the hydration number is $6/110 \times \frac{2c_{H_2O}}{c} = 6$.

D. The relation between water dynamics measured with THz-DR and fs-IR

A strong advantage of the fs-IR technique described above is that it is selectively sensitive to the reorientation of the water molecules in the system. A disadvantage is that we can only measure the anisotropy dynamics up to 10 ps after the pump excitation, because of the vibrational relaxation of the OD vibration. This relaxation has a typical time constant of 1.8 ps, making the signal too weak after 10 ps to determine its anisotropy. Hence, the technique can only be used to extract reorientation time scales that are within a 10 ps time window. Dielectric relaxation measurements are sensitive to a larger range of reorientation time scales – typically from sub-picosecond to microseconds. However this technique has a lower specific sensitivity as all electric field induced polarizations are probed that result from processes such as the reorientation of dipolar species and the movement of ionic charges. Therefore the techniques of dielectric relaxation and polarization-resolved pump-probe spectroscopy together are very powerful at studying reorientation dynamics over a range of time scales with high specificity.

In neat HDO:H$_2$O under ambient conditions, the time scale of the decay of the anisotropy ($\sim$2.5 ps) differs by a factor of 3.4 from the Debye relaxation time τ_D of pure water ($\sim$8.4 ps) [42]. This factor finds its origin in the different correlation function order that the measurement is sensitive to (first order for THz-DR and second order for fs-IR), and in the macroscopic nature of the THz-DR technique (which is sensitive to the polarization of all dipoles and charges in the sample) vs. the microscopic nature of the fs-IR technique (which probes well-separated HDO molecules in an H$_2$O matrix). The different order of the correlation function that is measured leads to a time scale for DR that is $2.5 - 3$ times longer than for fs-IR measurements [23]. The macroscopic nature of DR measurements furthermore requires taking into account the local field effects (molecules can experience a slightly different field than the applied external field) and dipole-dipole correlations (preferred parallel or anti-parallel orientations of neighboring molecules) as expressed through the static Kirkwood correlation factor g and the dynamic correlation factor $\dot{g}$ [2, 3, 29]. In neat water, these correlation effects are either small or nearly cancel each other, as the observed difference between the time constants is a factor of 3.4 [42].

In spite of the difference in measured time constants, the two techniques probe the same physical process: the reorientation of water molecules resulting from the collective reorganization of the liquid. With molecular dynamics simulation it was found that for pure water the reorientation occurs through a molecular jump mechanism [23, 25]. In this mechanism the orientation

angle of the OH groups of the water molecules does not change via many successive small steps, but rather via large angular jumps with a distribution of jump angles peaked at 50° [25]. It was shown by simulations that the same large-angle molecular jump mechanism applies to aqueous salt solutions [24], which was confirmed recently using polarization-selective two-dimensional infrared spectroscopy measurements [14].

III.   RESULTS AND DISCUSSION

A.   THz-DR results: LiCl vs. CsF

Figure 1 shows the results of the terahertz dielectric relaxation measurements of CsCl, LiCl and CsF. Here, CsCl is used as the calibration salt with known dielectric properties from Ref. [7] and the other salts consist of a strongly hydrated ion (Li$^+$ and F$^-$, resp.) combined with a weakly hydrated counterion (Cl$^-$ and Cs$^+$, resp.). The difference between the dielectric responses of LiCl and CsCl (measured in parallel) is larger than the difference between CsF and CsCl (measured in parallel). For LiCl, the permittivity difference becomes more negative for decreasing frequencies, clearly indicating that the static permittivity of LiCl is lower than that of pure water, i.e. indicating depolarization. This effect is much less pronounced for the CsF solution, where the real part of the permittivity difference is even slightly positive. These dielectric data thus indicate that the depolarization for LiCl is larger than for CsF and therefore that there is a larger fraction of slow water associated with dissolved LiCl than with dissolved CsF.

This qualitative conclusion is quantitatively confirmed when we calculate the slow water fraction, as described earlier (see Section II B 3), taking into account all effects that contribute to a modification of the dielectric response: the ion mobility, water molecules responding dynamically to the moving ions (kinetic depolarization) and the lower water concentration (dilution), thereby singling out the effect of the presence of slow hydration water. The ion mobility leads to an increase in the imaginary permittivity, whereas the other three effects lead to a decrease in overall permittivity (depolarization). Incidentally, for most salts in the THz region, the effects of ion mobility, kinetic depolarization and dilution nearly cancel each other, so that a direct interpretation of the measured dielectric responses in terms of the slowing down of the water reorientation is not unreasonable. This is especially the case for dissolved salts with very similar ion mobilities (as for CsF and LiCl). The extracted slow water fractions for LiCl and CsF as a function of concentration, after correction for all effects mentioned above, are shown in Fig. 2A. The linear slopes correspond to a hydration number of $N^{\mathrm{THz-DR}} \approx 8$ for LiCl and $N^{\mathrm{THz-DR}} \approx 2$ for CsF.
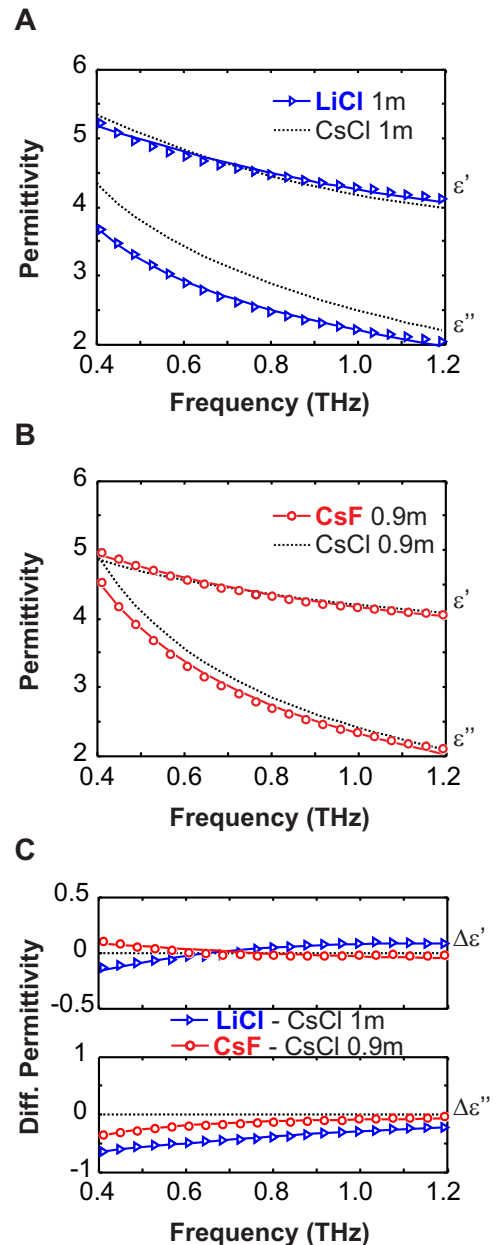

FIG. 1: The extracted dielectric function of LiCl compared to CsCl (**A**) and of CsF compared to CsCl (**B**). (**C**) The differential dielectric response of LiCl-CsCl (blue triangles) and of CsF-CsCl (red circles).

B.   fs-IR results: LiCl vs. CsF

Figure 3 shows the anisotropy decay as a function of time for LiCl and CsF up to a concentration of 4 mol/kg. As the anisotropy decay directly reflects the orientational dynamics of the water molecules, it is clear that there is a larger slow water fraction when

CsF is present than when LiCl is present. To quantify this effect, we describe the anisotropy decay with a biexponential function, as explained in Section II C 3. The extracted slow water fraction for LiCl and CsF as a function of concentration are shown in Fig. 2B. The linear slopes correspond to a hydration number of $N^{\text{fs}-\text{IR}} \approx$ 2 for LiCl and $N^{\text{fs}-\text{IR}} \approx 9$ for CsF, i.e. approximately the inverse result of that found by THz-DR spectroscopy.
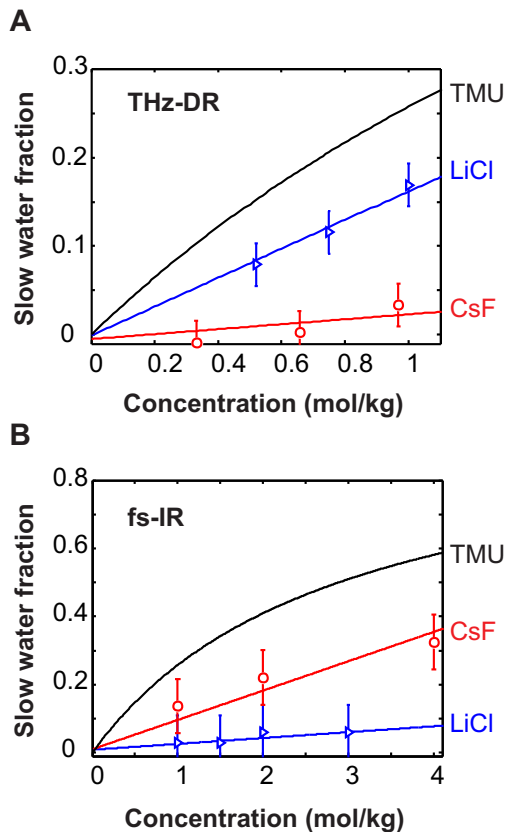

FIG. 2: Comparison of the fractions of slow hydration shell water for LiCl, CsF and TMU, as found by THz-DR (**A**) and fs-IR (**B**) spectroscopy. The TMU data are from Refs. [36] and [41] for the fs-IR and DR measurements, resp. Note that the two panels have different concentration ranges.

In our fs-IR measurements of orientational dynamics it is necessary to eliminate one effect that can lead to the observation of slow anisotropy decay. In Ref. [24], Laage et al. performed molecular dynamics simulations of aqueous NaCl solutions. They pointed out that fs-IR measurements at long delay times are biased to the OD groups that have intact hydrogen bonds with the chloride ions, as these OD-stretch vibrations have longer vibrational lifetimes. As these OD-groups have kept their hydrogen bonds to the chloride ions intact, they have probably not, or only partly reoriented, thus giving rise to a slow component in the anisotropy dynamics. In the measurements of LiCl solutions, we avoid this bias by using a red-shifted excitation and detection

pulse centered around 2480 cm^{-1}, which has limited spectral overlap with the blue-shifted OD-stretch modes of water molecules that are bound to chloride ions. In the case of CsF solutions we use the same excitation and detection spectrum, but now the OD-stretch mode of fluoride-bound water molecules is not blueshifted, so that we do probe their dynamics. We have verified that the vibrational lifetime of these OD-stretch modes of fluoride-bound water molecules have a similar absorption spectrum and vibrational lifetime as bulk and cation-bound water molecules (presumably due to the stronger hydrogen bonds between water and fluoride): The decay rates we obtain by describing the isotropic signals with a cascading model as in Ref. [34] are the same as for neat water and do not depend on CsF concentration. This means that the measured anisotropy dynamics represent the reorientation dynamics of the bulk water and water in the hydration shells of cesium and fluoride, without any bias for OD groups that keep their hydrogen bond intact.
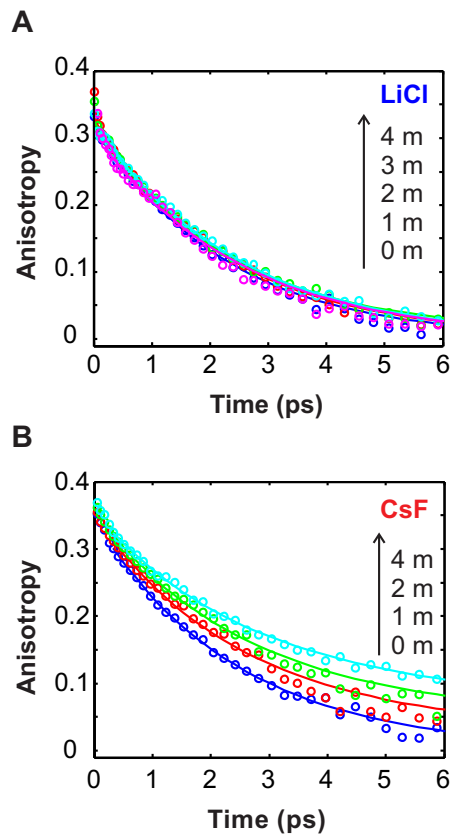

FIG. 3: The anisotropy decay, obtained with pump/probe frequency centered at 2480 cm^{-1}, as a function of delay time for different concentrations of LiCl (**A**) and CsF (**B**).

C. Anisotropic reorientation around ions: semi-rigid hydration

From Fig. 2 it is clear that the slow water fractions of LiCl and CsF are not the same, when measured with THz-DR and with fs-IR spectroscopy. THz-DR measures a larger slow water fraction for LiCl than for CsF, while in the fs-IR measurements it is exactly the opposite. To understand this discrepancy, we recall that THz-DR measurements are sensitive to the reorientation dynamics of the water dipole $\vec{p}$, whereas fs-IR measures the reorientation dynamics of the transition dipole moment $\vec{\mu}$ of the OD-vibration. These vectors point in a different direction, and thus the THz-DR and fs-IR measurements are consistent if the slowed down water molecules reorient in an anisotropic fashion. We thus conclude that solvated LiCl mainly slows down the dipole $\vec{p}$, but leaves the rotation of the OD and OH vectors (parallel with the transition dipole $\vec{\mu}$) largely unaffected. On the other hand, solvated CsF mainly slows down the rotation of the OH vector, while leaving the dipoles $\vec{p}$ unaffected.

To investigate the origin of the anisotropic reorientation, we compare the results for singly-charged solvated ions (Li^+, Cl^-, Cs^+ and F^-) with the solvation of the neutrally charged hydrophobic molecule tetramethylurea (TMU) in Fig. 2. It has been shown that TMU molecules significantly slow down a number of water molecules in their proximity, as evidenced by NMR [39], fs-IR [35, 36] and DR measurements in the MHz-THz range [41]. As shown above, the fs-IR and DR measurements provide distinctly different amounts of slow water for identical salts. In contrast, for TMU the two techniques reveal identical fractions of slow water around this neutral solute [41]. Hence, we conclude that the water molecules around TMU reorient slowly in an isotropic fashion. This is very different from the case of salts, where evidently the reorientation is anisotropic. This anisotropic reorientation of water in salt solutions is strongly connected to the electric fields exerted by the charges of the dissolved ions.

We can separate the effects of the solvated salts into the effects of their constituent ions. As smaller ions have a higher charge density, we can expect the largest effects to arise from Li^+ and F^-. Indeed these ions are known to be more strongly hydrated than Cl^- and Cs^+ [8]. The results for LiCl can thus be interpreted as follows. Water molecules around Li^+ have a fixed dipole vector, but can rotate their dipole moment, as shown schematically in Fig. 4. This is clearly the result of the local electric field around the positive ion, which makes water dipoles point radially away from the positive charge. For CsF the interaction is mainly due to the formation of directional hydrogen bonds between OD-groups and the negative charge of the F^- ion (the Cs^+ ion is very large, and has a correspondingly small
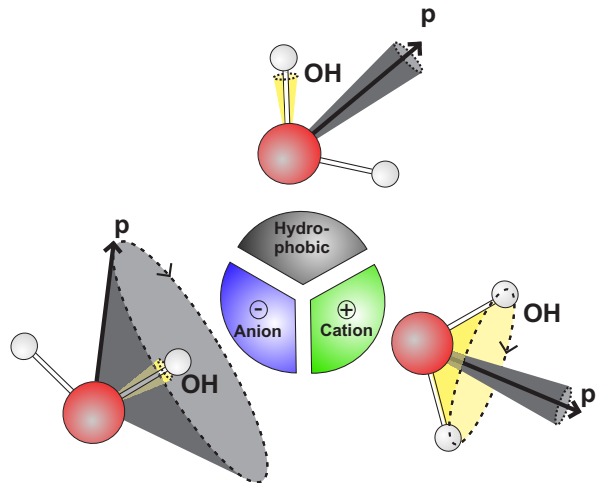

FIG. 4: Graphical representation of water dynamics around a cation (anisotropic reorientation: dipole $\vec{p}$ slowed), an anion (anisotropic reorientation: OD vector slowed), and a hydrophobe (isotropic reorientation: both vectors slowed).

charge density). Due to this strong hydrogen-bond interaction the reorientation of the OD groups pointing towards the F^- ion is strongly slowed down. In contrast, the dipole vector of the water to which the OD group belongs is hardly affected in its orientational mobility. This leads to a picture of 'semi-rigid hydration' of ions: the reorientation of water molecules is only affected along a certain vector, whereas reorientation in other directions remains largely unaffected. This picture holds true for the case where the solvated salt consists of a strongly hydrated ion with a weakly hydrated counterion.

The range of the semi-rigid hydration effect is restricted mainly to water molecules in the first solvation shell around the hydrated ions, as concluded from the hydration numbers of ~ 8 for Li^+ and F^-. Outside the first solvation shell, water molecules behave predominantly bulk-like. In the semi-rigid hydration picture, only one OD-group per water molecule is affected by the anion (the one that points to the anion). It is possible that some water molecules form two hydrogen bonds with a negatively charged ion. In this case, the hydration number N^{fs-IR} derived from the fs-IR data would be too large, as in the calculation of N^{fs-IR} from f_{slow}^{fs-IR} it is assumed that the two slow OD groups belong to two different water molecules. The doubly bonded water molecules would also contribute to the hydration number determined with DR, as the dipole vector will be fixed as well in that case. The observed THz-DR hydration number of $N^{THz-DR} \approx 2$ for CsF could be partly due to this type of doubly bonded water molecules. However, the low value of of the hydration number also implies that most water molecules do not form such double hydrogen bonds with the F^- ion.

The present picture of semi-rigid hydration implies

that the two techniques have complementary sensitivities for hydration effects around charged species: dielectric relaxation spectroscopy is most sensitive to hydration effects around positive charges, whereas femtosecond infrared spectroscopy is most sensitive to hydration effects around negative charges. Indeed DR measurements in the MHz-GHz range revealed that hydration numbers depend strongly on the cation, according to the sequence $MgCl_2 >$ LiCl > NaCl > KCl, CsCl (Refs. [1, 6, 7, 45] respectively). On the other hand, there was almost no dependence on the nature of the anion for NaBr, NaI, $NaNO_3$, $NaClO_4$ and NaSCN [46]. The same holds for THz-DR measurements on $MgClO_4$, LiCl, NaCl, Cs_2SO_4 and CsCl, which showed clearly dominant cation hydration effects [40]. Turning to fs-IR measurements, it was shown that for NaCl, NaBr and NaI the slowdown of the reorientation dynamics is dependent on the nature of the anion [20], whereas measurements on $Mg(ClO_4)_2$ and $NaClO_4$ showed no sensitivity towards the cation; water is slowed only for first solvation shell water molecules around the ClO_4^- anion [19, 33]. Furthermore, fs-IR measurements showed a negligible hydration effect around the cations for LiI salts up to 4 mol/kg [40]. All these previous studies are fully consistent with the unifying picture of semi-rigid ion hydration presented in Fig. 4. From the theory side, we find support for our finding that the range of the semi-rigid hydration effect is restricted to the first solvation shell, as shown for NaBr solutions [26].

The semi-rigid hydration around cations and anions is valid for salts that comprise a strongly hydrated ion with a weakly hydrated counterion. In the case where strongly hydrated cations and anions are combined - such as $MgSO_4$ and Na_2SO_4 - cooperative effects lead to more rigid hydration structures with large values for both N^{THz-DR} and N^{fs-IR}, as discussed in Ref. [40]. These rigid hydration structures probably arise as a result of the combination of a strong fixing of the dipole vectors $\vec{p}$ by the cations and a strong fixing of the direction of the hydroxyl groups by the anions. In addition, ion pairing effects may play a role (especially at lower concentrations) [5], leading to the formation of structures in which the cation and anion are separated by a limited number of water layers that together form a locked hydrogen-bonded structure.

D. The combination of weakly hydrated cations and anions: CsI

A third type of salts consists of cations and anions that are both weakly hydrated. These salts have been denoted as 'structure breaking' or 'chaotropic' salts, suggesting that the ions would weaken the hydrogen-bond structure of liquid water. Here, we study this case by examining the hydration effects of the salt CsI. We show the dielectric responses for CsI and CsCl in Fig. 5A, where CsCl is again used as the calibration salt with known dielectric properties and with a negligibly small hydration number [7]. Clearly, the dielectric properties of CsI and CsCl are almost identical, with only minor differences that arise from the slightly higher conductivity of CsI and a Debye reorientation time that decreases more strongly with concentration for I^- than for Cl^-, as is known from Ref. [46]. Taking these effects into account as explained in Section II B 3, we find the slow water fraction of CsI shown in Fig. 5B. Clearly, there is a negligible slow water fraction in aqueous solutions of CsI.
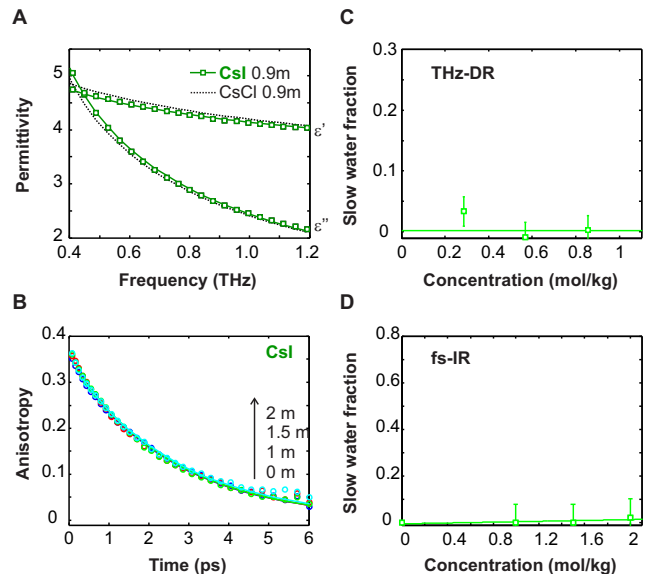

FIG. 5: Dielectric response of CsI compared to CsCl (**A**) and extracted slow water fraction according to THz-DR, with the same vertical range as in Fig. 2A (**B**). Anisotropy decay, obtained with pump/probe frequency centered at $2480 \ cm^{-1}$, for different concentrations of CsI (**C**) and the extracted slow water fraction according to fs-IR with the same vertical range as in Fig. 2B (**D**).

To investigate this 'structure breaking' salt further, we show the anisotropy decay for different concentrations of CsI solutions in water (Fig. 5C), measured with fs-IR pump-probe spectroscopy. Here, we use a similarly red-shifted pump/probe spectrum as for LiCl and CsF, so that we do not probe OD's that are weakly hydrogen-bonded to iodide (to avoid a possible bias due to longer lifetimes of these OD's, as explained above and in Ref. [24]). The anisotropy decay therefore reflects the dynamics of water molecules in the first hydration shell of the Cs^+ cation and all water molecules outside of the first hydration shells of the cation and the anion. These anisotropy decays can be described very well with a large fraction of water molecules with the same reorientation time as neat water and a very small fraction of slower water, in excellent agreement with the THz-DR results, where also a negligibly small slow water fraction was

found. This is shown in Fig. 5D, where we show the fraction of slow water as a function of CsI concentration, which is negligibly small for all concentrations. This means that the reorientation of water in this solution (besides water in the shell of the anion, which we do not probe) behaves very similar to bulk water. The fs-IR measurements furthermore show that there is no evidence for a speedup of the water dynamics, i.e. no evident 'structure breaking' effect.

IV. CONCLUSIONS

We studied the orientational dynamics of water molecules hydrating three different types of salts with terahertz dielectric relaxation spectroscopy and femtosecond infrared pump-probe spectroscopy. The studied salt types comprise *(i)* a strongly hydrated ion with a weakly hydrated counterion, *(ii)* a strongly hydrated ion with a strongly hydrated counterion, and *(iii)* a weakly hydrated ion with a weakly hydrated counterion. It turns out that in the case of type *(i)*, the dynamics of water molecules around the ions are best described as semi-rigid. In this semi-rigid hydration picture, cations slow down the reorientation dynamics of the water dipole vectors and anions slow down the reorientation dynamics of the OD-groups pointing to the anion.

This anisotropic reorientation behavior around ions is clearly distinct from the isotropic effects of hydrophobic molecular groups on the reorientation.

The semi-rigid hydration effect is largely restricted to the first hydration shell of the ions. Hence, for the case of salts that consist of a strongly hydrated ion and a weakly hydrated counterion, there is no long-range ion-water interaction effect. This contrasts with salts consisting of ions and counterions that are both strongly hydrated, type *(ii)*, for which the effects extend well beyond the first hydration shell, as demonstrated in Ref. [40]. Finally, for a combination of a weakly hydrated ion with a weakly hydrated counterion, type *(iii)*, we find that the local water molecular reorientation neither slows down nor speeds up. This result shows that there is no structure breaking effect in this type of salt solutions.

[1] J. Barthel, H. Hetzenauer, and R. Buchner. Dielectric-relaxation of aqueous-electrolyte solutions .1. solvent relaxation of 1/2, 2/1, and 2/2 electrolyte-solutions. Berichte der Bunsen-Gesellschaft- Physical Chemistry Chemical Physics, 96:988–997, 1992.

[2] C.J.F.B. Böttcher. Theory of Electrical Polarization Vol. I. Elsevier (Amsterdam), 1973.

[3] C.J.F.B. Böttcher and R. Bordewijk. Theory of Electrical Polarization Vol. II. Elsevier (Amsterdam), 1978.

[4] R. Buchner, J. Barthel, and J. Stauber. The dielectric relaxation of water between 0 °C and 35 °C. Chem. Phys. Lett., 306:57–63, 1999.

[5] R. Buchner, T. Chen, and G. Hefter. Complexity in "simple" electrolyte solutions: Ion pairing in $MgSO_4$(aq). J. Phys. Chem. B, 108:2365–2375, 2004.

[6] R. Buchner, G. Hefter, and P.M. May. Dielectric relaxation of aqueous NaCl solutions. J. Phys. Chem. A, 103:1–9, 1999.

[7] T. Chen, G. Hefter, and R. Buchner. Dielectric spectroscopy of aqueous solutions of KCl and CsCl. J. Phys. Chem. A, 107:4025–4031, 2003.

[8] F. Franks, editor. Water: A Comprehensive Treatise, volume 3. Plenum, London, 1973.

[9] T. Fukasawa, T. Sato, J. Watanabe, Y. Hama, W. Kunz, and R. Buchner. Relation between dielectric and low-frequency raman spectra of hydrogen-bond liquids. Phys. Rev. Lett., 95:197802, 2005.

[10] I.A. Heisler and S.R. Meech. Low-frequency modes of aqueous alkali halide solutions: Glimpsing the hydrogen bonding vibration. Science, 327:857–860, 2010.

[11] M. Heyden, J. Sun, S. Funkner, G. Mathias, H. Forbert, M. Havenith, and Marx D. Dissecting the thz spectrum of liquid water from first principles via correlations in time and space. Proc. Natl. Acad. Soc. USA, 107:12068–12073, 2010.

[12] F. Hofmeister. Zur Lehre von der Wirkung der Salze. Arch. Exp. Pathol. Pharmakol., 24:247–260, 1888.

[13] K.-L. Hsia and R. M. Fuoss. Conductance of the alkali halides. xi. cesium bromide and iodide in water at 25.deg. J. Am. Chem. Soc., 90:3055–3060, 1968.

[14] M. Ji, M. Odelius, and K. J. Gaffney. Large angular jump mechanism observed for hydrogen bond exchange in aqueous perchlorate solution. Science, 328:1003–1005, 2010.

[15] U. Kaatze. The dielectric properties of water in its different states of interaction. J. Sol. Chem., 26:1049–1112, 1997.

[16] J. T. Kindt and C. A. Schmuttenmaer. Far-infrared dielectric properties of polar liquids probed by femtosecond terahertz pulse spectroscopy. J. Phys. Chem., 100(24):10373–10379, January 1996.

[17] J. Knab, J.Y. Chen, and A. Markelz. Hydration dependence of conformational dielectric relaxation of lysozyme. Biophys. J., 90:2576–2581, 2006.

[18] S. Koneshan, J.C. Rasaiah, R.M. Lynden-Bell, and S.H. Lee. Solvent structure, dynamics, and ion mobility in aqueous solutions at 25 °C. J. Phys. Chem. B, 102:4193–4204, 1998.

[19] M. F. Kropman and H. J. Bakker. Femtosecond mid-infrared spectroscopy of aqueous solvation shells. J. Chem. Phys., 115(19):8942–8948, 2001.

[20] M. F. Kropman, H.-K. Nienhuys, and H. J. Bakker. Real-time measurement of the orientational dynamics of aqueous solvation shells in bulk liquid water. Phys. Rev. Lett., 88:077601, 2002.

[21] W. Kunz. Specific ion effects in colloidal and biological systems. Curr. Opin. Colloid Interface, 15:34–39, 2010.

[22] W. Kunz, J. Henle, and B.W. Ninham. 'Zur Lehre von der Wirkung der Salze' (about the science of the effect of salts): Franz Hofmeister's historical papers. Curr. Opin. Colloid Interface, 9:19–37, 2004.

[23] D. Laage and J.T. Hynes. A molecular jump mechanism of water reorientation. Science, 311:832–835, 2006.

[24] D. Laage and J.T. Hynes. Reorientational dynamics of water molecules in anionic hydration shells. Proc. Natl. Acad. Soc. USA, 104:11167–11172, 2007.

[25] D. Laage and J.T. Hynes. On the molecular mechanism of water reorientation. J. Phys. Chem. B, 112:14230–14242, 2008.

[26] Y.A. Lin, B.M. Auer, and J.L. Skinner. Water structure, dynamics, and vibrational spectroscopy in sodium bromide solutions. J. Chem. Phys., 131:144511, 2009.

[27] D. V. Loginova, A. S. Lileev, and A.K. Lyashchenko. Microwave dielectric properties of aqueous solutions of potassium and cesium fluorides. Russian Journal of Physical Chemistry, 80:1626–1633, 2006.

[28] J. J. Loparo, C. J. Fecko, J. D. Eaves, S. T. Roberts, and A. Tokmakoff. Reorientational and configurational fluctuations in water observed on molecular length scales. Phys. Rev. B, 70:180201, 2004.

[29] P. Madden and D. Kivelson. Adv. Chem. Phys., 56:467, 1984.

[30] Y. Marcus. Effect of ions on the structure of water: Structure making and breaking. Chem. Rev., 109:1346–1370, 2009.

[31] D.E. Moilanen, E.E. Fenn, Y. Lin, J.L. Skinner, B. Bagchi, and M.D. Fayer. Water inertial reorientation: Hydrogen bond strength and the angular potential. Proc. Natl. Acad. Soc. USA, 105:5295–5300, 2008.

[32] D.E. Moilanen, D. Wong, D.E. Rosenfeld, E.E. Fenn, and M.D. Fayer. Ion-water hydrogen-bond switching observed with 2D IR vibrational echo chemical exchange spectroscopy. Proc. Natl. Acad. Soc. USA, 106:375–380, 2009.

[33] A.W. Omta, A.M. Kropman, S. Woutersen, and H.J. Bakker. Negligible effect of ions on the hydrogen-bond structure in liquid water. Science, 301:347–349, 2003.

[34] Y.L.A. Rezus and H.J. Bakker. On the orientational relaxation of HDO in liquid water. J. Chem. Phys., 123:114502, 2005.

[35] Y.L.A. Rezus and H.J. Bakker. Observation of immobilized water molecules around hydrophobic groups. Phys. Rev. Lett., 99:148301, 2007.

[36] Y.L.A. Rezus and H.J. Bakker. Strong slowing down of water reorientation in mixtures of water and tetramethylurea. J. Phys. Chem. A, 112:2355–2361, 2008.

[37] C. Rønne, L. Thrane, P.O. Astrand, A. Wallqvist, K.V. Mikkelsen, and S.R. Keiding. Investigation of the temperature dependence of dielectric relaxation in liquid water by THz reflection spectroscopy and molecular dynamics simulation. J. Chem. Phys., 107:5319–5331, 1997.

[38] D.A. Schmidt, Ö. Birer, S. Funkner, B.P. Born, R. Gnanasekaran, G.W. Schwaab, D.M. Leitner, and M. Havenith. Rattling in the cage: Ions as probes of sub-picosecond water network dynamics. J. Am. Chem. Soc., 131:18512–18517, 2009.

[39] A. Shimizu, K. Fumino, K. Yukiyasu, and Y. Taniguchi. NMR studies on dynamic behavior of water molecule in aqueous denaturant solutions at 25 °C: Effects of guanidine hydrochloride, urea and alkylated ureas. J. Mol. Liq., 85:269–278, 2000.

[40] K.J. Tielrooij, N. Garcia-Araez, M. Bonn, and H.J. Bakker. Cooperativity in ion hydration. Science, 328:1006–1009, 2010.

[41] K.J. Tielrooij, J. Hunger, R. Buchner, M. Bonn, and H.J. Bakker. Influence of concentration and temperature on the dynamics of water in the hydrophobic hydration shell of tetramethylurea. J. Am. Chem. Soc., 132:15671–15678, 2010.

[42] K.J. Tielrooij, C. Petersen, Y.L.A. Rezus, and H.J. Bakker. Reorientation of HDO in liquid H_2O at different temperatures: Comparison of first and second order correlation functions. Chem. Phys. Lett., 471:71–74, 2009.

[43] K.J. Tielrooij, R.L.A. Timmer, H.J. Bakker, and M. Bonn. Structure dynamics of the proton in liquid water probed with terahertz time-domain spectroscopy. Phys. Rev. Lett., 102:198303, 2009.

[44] D.J. Tobias and J.C. Hemminger. Chemistry - getting specific about specific ion effects. Science, 319:1197, 2008.

[45] W. Wachter, S. Fernandez, R. Buchner, and G. Hefter. Ion association and hydration in aqueous solutions of LiCl and Li_2SO_4 by dielectric spectroscopy. J. Phys. Chem. B, 111:9010–9017, 2007.

[46] W. Wachter, W. Kunz, R. Buchner, and G. Hefter. Is there an anionic Hofmeister effect on water dynamics? Dielectric spectroscopy of aqueous solutions of NaBr, NaI, $NaNO_3$, $NaClO_4$, and NaSCN. J. Phys. Chem. A, 109:8675–8683, 2005.

[47] S. Woutersen, U. Emmerichs, and H.J. Bakker. Femtosecond mid-IR pump-probe spectroscopy of liquid water: Evidence for a two-component structure. Science, 278:658–660, 1997.

[48] H. Yada, M. Nagai, and K. Tanaka. Origin of the fast relaxation component of water and heavy water revealed by terahertz time-domain attenuated total reflection spectroscopy. Chem. Phys. Lett., 464:166–170, 2008.

[49] Y.J. Zhang and P. Cremer. Interactions between macromolecules and ions: the hofmeister series. Curr. Opin. Chem. Biol., 10:658–663, 2006.

[50] In his original work (published at the end of the 19th century), Franz Hofmeister described the effect of *salts* on biological solutions. The interpretation in terms of the effect of *individual ions* was given later, as also discussed in Ref. [21]

A1. APPENDIX: EXTRACTION OF THE CALIBRATED THZ DIELECTRIC RESPONSE

The extraction of the dielectric response in the case of liquid samples requires three measurements: THz electric field traces transmitted through air $E_{\mathrm{air}}(t)$, through an empty cuvette $E_{\mathrm{cuv}}(t)$, and through a cuvette filled with sample $E_{\mathrm{sam}}(t)$. The comparison of the first two measurements yields the dielectric properties of the cuvette. These are needed for the comparison of the last two measurements, and to obtain the dielectric properties of the sample. When the three measurements are executed in a consecutive manner, changes in laser output power, laser pointing, ambient temperature and sample alignment will result in an increasing uncertainty in the measured THz electric field transmission and hence the extracted dielectric response of the sample. Therefore we measure two samples in parallel, where one is a reference sample with known dielectric properties and the other is the sample whose dielectric response we want to obtain. To this end, we employ a mechanical device that enables measurements for the positions **L** and **R** within a duty cycle of 4 seconds. This method strongly reduces uncertainties and provides a means to calibrate the extracted dielectric response. We will first explain how the *measurements* are carried out, then the *extraction* procedures are explained, followed by a discussion of the *calibration* method.

Measurements – In the first measurement step, the traces $E_{\mathrm{air,L}}(t)$ and $E_{\mathrm{air,R}}(t)$ are measured, i.e. the THz traces transmitted through air, with the mechanical device in the left or right position. Here, each THz trace has a length of 5 ps, measured with steps of 50 fs (set by the delay of the 800 nm detection pulse with respect to the THz pulse) and each data point is averaged for 100 ms (100 laser shots). For each delay, the THz transmission for the L and R positions is measured, before the delay moves to the next point. The difference between the THz transmission $E_{\mathrm{air,L}}(t)$ and $E_{\mathrm{air,R}}(t)$ is typically less than 0.1%, as it is only determined by changes in THz intensity that occur during the 4 second duty cycle. In the second measurement step, the THz transmission through the left cuvette $E_{\mathrm{cuv,L}}(t)$ and through the right cuvette $E_{\mathrm{cuv,R}}(t)$ are measured. These two measurements will differ slightly, due to differences in the dielectric properties and the thicknesses of the cuvettes ($100 \pm 5\mu$m). In the third measurement step, we measure the THz transmission through the (reference) sample $E_{\mathrm{sam}}(t)$, where one cuvette contains the reference sample and the other cuvette the sample. Figure A1A shows the THz traces that correspond to $E_{\mathrm{air}}(t)$, $E_{\mathrm{cuv}}(t)$ and $E_{\mathrm{sam}}(t)$ for the L and R positions.

Extraction – We perform the analysis of the THz traces in the frequency domain for a number of chosen frequencies ν_{k}, taking into account all reflections r, transmissions t and phase changes P that occur as the THz field prop-
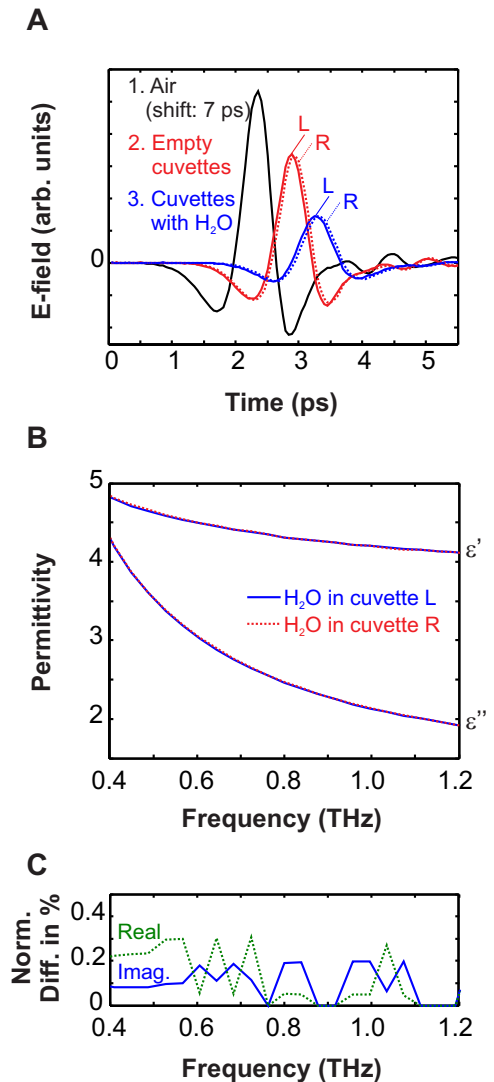

FIG. A1: **(A)** Transmitted electric field of THz pulses that have passed through air (shifted by 7 ps), through empty cuvettes and through a cuvette with water. **(B)** The extracted complex dielectric functions of water, according to the left measurement (blue connected line) and the right measurement (red dotted line). **(C)** The relative difference between the two measurements as a function of frequency.

agates:

$$r_{ij} = \frac{\hat{n}_j - \hat{n}_i}{\hat{n}_i + \hat{n}_j} \tag{A1}$$

$$t_{ij} = \frac{2\hat{n}_i}{\hat{n}_i + \hat{n}_j} \tag{A2}$$

$$P_{i,L_i} = e^{-i\hat{n}_i 2\pi\nu_{\mathrm{k}} L_i/c} \ , \tag{A3}$$

where $\hat{n}_i$ and $\hat{n}_j$ are the complex refractive indices of the media i and j, respectively; L_i the length of medium i and c the speed of light. In the first measurement step - with only the medium air - just a phase change occurs.

In the second measurement step, the THz light traverses five media, namely 1:A, 2:Q, 3:A, 4:Q and 5:A, with A air and Q quartz. This is the same in the third measurement step, except for medium 3, which is then either the sample or the reference sample, denoted as S. The comparison of the first two measurements - for both positions L and R - now gives

$$\frac{E_{\mathrm{cuv}}(\nu_k)}{E_{\mathrm{air}}(\nu_k)} = \frac{t_{AQ}P_{Q,L_2}t_{QA}P_{A,L_3}t_{AQ}P_{Q,L_4}t_{QA}}{1+r_{QA}r_{AQ}P_{A,L_3}^2} \times$$
$$\frac{1}{P_{A,L_2+L_3+L_4}} \quad , \text{ (A4)}$$

where the denominator of the first factor of equation (A4) accounts for multiple reflections in medium 3, which is necessary when the optical path length (here $L_3 = 100$ μm) is of the order of the THz wavelength or shorter. The only unknown parameter in this equation is the complex refractive index of the cuvettes $\hat{n}_Q = \hat{n}_2 = \hat{n}_4$, which we obtain by fitting Eq. A4 to the measured ratio $\frac{E_{\mathrm{cuv}}(\nu_k)}{E_{\mathrm{air}}(\nu_k)}$. Similarly, we use

$$\frac{E_{\mathrm{sam}}(\nu_k)}{E_{\mathrm{cuv}}(\nu_k)} = \frac{t_{QS}P_{S,L_3}t_{SQ}}{1+r_{QS}r_{SQ}P_{S,L_3}^2} \times$$
$$\frac{1+r_{QA}r_{AQ}P_{A,L_3}^2}{t_{QA}P_{A,L_3}t_{AQ}} \quad , \tag{A5}$$

to determine the last unknown parameter: the complex refractive index of the sample $\hat{n}_S = \hat{n}_3$. As we do this for a range of frequencies ν_k, this yields the frequency-dependent complex refractive index of the sample or the reference sample. To get an indication of the accuracy of the THz technique and the extraction procedure, we have measured two identical samples of pure liquid H_2O, each contained in one of the cuvettes during the third measurement step (see Fig. A1). These measurements show that the extracted refractive indices differ by less than 0.3%, as evidenced by Fig. A1C.

Calibration – Although the extracted refractive indices (or dielectric functions) of two identical samples are in excellent agreement with each other, it is still possible that the *absolute* refractive indices suffer from a systematic error. Since the systematic error is the same for the sample in position L and the sample in position R, we use a reference sample (CsCl) with known dielectric properties (from Ref. [7]) to calibrate the dielectric response of the sample. In the case of aqueous salt solutions, we describe both samples using a double-Debye dielectric relaxation model

$$\epsilon_{\mathrm{ref}}(\nu) = \frac{S_1}{1+i2\pi\nu\tau_{\mathrm{D}}} + \frac{S_2}{1+i2\pi\nu\tau_2} + \frac{\sigma}{i2\pi\nu\epsilon_0} + \epsilon_\infty \text{ (A6)}$$

where the first term describes the dielectric relaxation mode with relaxation strength $S_1 = \epsilon_{\mathrm{s}} - \epsilon_1$ and (Debye) reorientation time τ_{D}. The second mode has a (much smaller) relaxation strength $S_2 = \epsilon_1 - \epsilon_\infty$ and reorientation time τ_2. For pure water, the slow Debye mode is centered around 20 GHz, whereas the faster mode is located around 0.6 THz. The last term of equation (A6) describes the contribution to the dielectric response of the ion conductivity σ. To reduce the number of fit parameters, we fix the static dielectric constant for the reference sample $\epsilon_{\mathrm{s}}^{\mathrm{ref}}$ to its literature value and use literature data for σ^{ref}, both from Ref. [7]. The resultant Debye relaxation time $\tau_{\mathrm{D}}^{\mathrm{ref}}$ is then used as the calibration parameter for the sample, by describing the dielectric response of the sample with Eq. A6 with $\tau_{\mathrm{D}}^{\mathrm{sam}} = \tau_{\mathrm{D}}^{\mathrm{ref}}$ and literature data for σ^{sam}. This results in the calibrated relaxation strengths S_1^{sam} and S_2^{sam}, which contain the information on the fraction of water molecules with bulk-like reorientation dynamics.

The explicit assumption in this procedure is that the reference sample has the same Debye relaxation time as the sample under study. This requirement can be met by using the same anion with the same concentration for both samples, as the Debye time weakly depends on concentration and the nature of the anion [46]. In the case of different anions and/or different concentrations for sample and reference sample, we perform the calibration routine using the following concentration-dependent Debye times: $\tau_{\mathrm{D}}(c) = \tau_{\mathrm{D}}(0) - b \cdot c$, with $b = 0.2$, 0.5 and 1 s·L/mol for the anions F^- [27], Cl^- [46] and I^- [46], respectively. Finally, we note that the calibration routine requires that there are no other modes, such as ion pair contributions, active in our measurement window of 0.4-1.2 THz. This is usually the case, as the ion pair dipoles typically reorient significantly more slowly than water dipoles, due to the much larger size of the ion pair complex.